Analytical Biochemistry 502 (2016) 24–35

Contents lists available at ScienceDirect

Analytical Biochemistry

journal homepage: www.elsevier.com/locate/yabio

Homogeneous time-resolved G protein-coupled receptor–ligand binding assay based on fluorescence cross-correlation spectroscopy

Thomas Antoine [a, 1], David Ott [a, 1], Katharina Ebell [a], Kerrin Hansen [a], Luc Henry [b], Frank Becker [a], Stefan Hannus [a, *]

[a] Intana Bioscience, DE-82152, Planegg/Martinsried, Germany
[b] Laboratory of Protein Engineering, Swiss Federal Institute of Technology Lausanne (EPFL), CH-1015 Lausanne, Switzerland

ARTICLE INFO

Article history:
Received 18 December 2015
Received in revised form
19 February 2016
Accepted 25 February 2016
Available online 4 March 2016

Keywords:
GPCR
Homogeneous time-resolved binding assay
Fluorescence correlation spectroscopy
Fluorescence cross-correlation spectroscopy
Affinity determination
Binding kinetics

ABSTRACT

G protein-coupled receptors (GPCRs) mediate many important physiological functions and are considered as one of the most successful therapeutic target classes for a wide spectrum of diseases. Drug discovery projects generally benefit from a broad range of experimental approaches for screening compound libraries and for the characterization of binding modes of drug candidates. Owing to the difficulties in solubilizing and purifying GPCRs, assay formats have been so far mainly limited to cell-based functional assays and radioligand binding assays. In this study, we used fluorescence cross-correlation spectroscopy (FCCS) to analyze the interaction of detergent-solubilized receptors to various types of GPCR ligands: endogenous peptides, small molecules, and a large surrogate antagonist represented by a blocking monoclonal antibody. Our work demonstrates the suitability of the homogeneous and time-resolved FCCS assay format for a robust, high-throughput determination of receptor–ligand binding affinities and kinetic rate constants for various therapeutically relevant GPCRs.

G protein-coupled receptors (GPCRs), also known as seven-transmembrane receptors, are the largest family of cell surface receptors. They are activated by a wide variety of stimulants, including light odorant molecules, peptide and nonpeptide neurotransmitters, hormones, growth factors, and lipids. GPCRs control a wide variety of physiological processes, including sensory transduction, cell–cell communication, neuronal transmission, and hormonal signaling [1]. Due to a high potential for GPCR-specific therapeutic interventions using small molecules or peptidomimetics, GPCRs became the largest family of drug targets. These receptors are the target of 40–50% of the current therapeutic agents on the market. Therefore, development of GPCR assays and ligand screening remain the major focus of drug discovery research worldwide [2–9].

Currently available assays to assess GPCR–ligand binding affinity, specificity, and potency fall into two main categories: (i) assays where binding of radioactively or fluorescently labeled ligands directly to a specific GPCR is measured [10–15] and (ii) cell-based functional assays that measure downstream effects of ligand–receptor interaction (numerous events in the signal transduction cascade have been used for this purpose, e.g., intracellular accumulation of inositol 1,4,5-triphosphate or cAMP and release of Ca^{2+} ions into the cytosol) [16]. An ideal ligand binding assay should be simple, robust, homogeneous and hence amenable to automation, and it should allow acquisition of time-resolved data for determination of kinetic parameters.

For determination of GPCR–ligand affinities, fluorescence correlation spectroscopy (FCS) and fluorescence cross-correlation spectroscopy (FCCS) are attractive alternatives to other homogeneous fluorescent techniques such as time-resolved fluorescence resonance energy transfer (TR–FRET) [4,17]. In FCS, information on the mobility and concentration of molecules is obtained from an analysis of fluorescence fluctuations, caused by diffusion of

Abbreviations used: GPCR, G protein-coupled receptor; FCS, fluorescence correlation spectroscopy; FCCS, fluorescence cross-correlation spectroscopy; TR–FRET, time-resolved fluorescence resonance energy transfer; NTR1, neurotensin receptor type 1; ADRB2, β2-adrenergic receptor; CXCR4, C-X-C chemokine receptor type 4; NT, neurotensin (8–13); SDF1α, stromal cell-derived factor 1; ORF, open reading frame; PCR, polymerase chain reaction; PEG4, 4-polyethylene glycol spacer; DMSO, dimethyl sulfoxide; RT, room temperature; PBS, phosphate-buffered saline; DOL, degree of labeling; DDM, *n*-dodecyl β-D-maltoside; CHS, cholesteryl hemisuccinate; AF647, AlexaFluor 647; PMT, photomultiplier tube; APD, avalanche photodiode; HTS, high-throughput screening; SPR, surface plasmon resonance.

* Corresponding author.
E-mail address: stefan.hannus@intana.de (S. Hannus).

[1] These authors contributed equally to this work.

http://dx.doi.org/10.1016/j.ab.2016.02.017

fluorescently labeled molecules through a subfemtoliter confocal detection volume. In FCCS, concerted fluorescence fluctuations, caused by co-diffusion of two spectrally well-separated fluorophores, are detected [18]. Contrary to FRET, the signal in FCCS does not depend on the distance of fluorophores. Therefore, there are no constraints on the use of a flexible linker between a fluorophore and a GPCR-specific probe. With sensitivity in the subnanomolar range, FCS has become an important tool to address molecular dynamics and interactions in cells and subcellular compartments [19].

Here we report the first successful application of FCCS for a high-throughput determination of affinity between recombinantly expressed GPCRs and their ligands (agonists or antagonists). Equilibrium thermodynamic parameters (K_D/K_I values) were determined for three distinct examples of human GPCRs: neurotensin receptor type 1 (NTR1), β2-adrenergic receptor (ADRB2), and C-X-C chemokine receptor type 4 (CXCR4). Furthermore, in this study we show examples that also kinetic parameters (k_{on}/k_{off}) for a fluorescently labeled probe, as well as for unlabeled compounds (henceforth "competitors"), can be readily determined by FCCS. FCCS used in the presented format is simple, reliable, and rapid. It requires minimal sample preparation and minute sample volumes, and it can be easily automated.

Materials and methods

Materials

Reagents were obtained from Anatrace (Maumee, OH, USA), AppliChem (Darmstadt, Germany), Carl Roth (Karlsruhe, Germany), or Sigma–Aldrich (St. Louis, MO, USA) unless stated otherwise. Unlabeled compounds were purchased from Tocris (Bristol, UK) or Abcam (Cambridge, UK) with the exception of (−)-norepinephrine and SR48692 (Sigma–Aldrich), SR 142948A (Santa Cruz Biotechnology, Santa Cruz, CA, USA), neurotensin (8–13) (NT; AnaSpec/MoBiTec, Goettingen, Germany), and TC 14012 (Cayman Chemical, Ann Arbor, MI, USA). Anti-CXCR4 monoclonal antibody clone 44708 (murine IgG2A; cat. no. MAB171) was acquired from R&D Systems (Minneapolis, MN, USA). Unlabeled recombinant hCXCL12/SDF-1α was obtained as a gift from Annette Beck-Sickinger (Institut für Biochemie, Universität Leipzig, Germany). Human synthetic stromal cell-derived factor 1 (SDF1α) labeled specifically on residue Lys64 with AlexaFluor 647 (henceforth "SDF1α-AF647"; cat. no. CAF-11) was acquired from Almac (Craigavon, UK).

Human GPCR variants

The open reading frame (ORF) of selected wild-type GPCRs was polymerase chain reaction (PCR) amplified from a plasmid DNA encoding a particular receptor and subcloned into a mammalian expression vector pCGTO in frame with a C-terminal fusion partner (GFP) and a short linker (KLGGG) in between the GPCR and GFP. The GFP used in this study is an enhanced GFP with two mutations (Phe64Leu and Ser65Thr) [20] and was subcloned into the vector pCGTO from pEGFP-N1 (Clontech, Mountain View, CA, USA). Internal restriction sites (e.g., *Eco*RI and *Hin*dIII) that could interfere with the plasmid construction were removed from the ORFs by PCR, with reverse complementary primer pairs introducing the required silent mutations. The cloned GPCRs were human β2 adrenergic receptor (UniProt ID: P07550), human neurotensin receptor type 1 (UniProt ID: P30989), and human C-X-C chemokine receptor type 4 (UniProt ID: P61073). Based on previously reported engineered variants of rat NTR1 with substantially improved thermostability in detergents [21,22], we also constructed mutated variants of human NTR1: single mutants Ala85Leu, Ile252Ala, and Phe353Val and triple mutant "TTM," which combines the three single mutations A85L$^{1.54}$, I252A$^{5.54}$, and F353V$^{7.42}$.

Fluorescent labeling of neurotensin (8–13)

The hexapeptide neurotensin (8–13) is an active fragment of neurotensin, and it has been shown that the modification of neurotensin (8–13) (henceforth "NT") on its N terminus does not affect its affinity to NTR1 [23]. NT was coupled via its primary NH_2 group to DY-647-PEG4 as follows. First, 300 nmol (245 μg) of NT and 198 nmol (200 μg) of DY-647-NHS ester carrying a 4-polyethylene glycol spacer (PEG4; Dyomics, Jena, Germany) were dissolved and mixed in a total of 80 μl dimethyl sulfoxide (DMSO). On the addition of 0.7 μl *N,N*-diisopropylethylamine, the mixture was incubated in the dark at room temperature (RT) for 20 h. The reaction was stopped by the addition of 160 μl dH_2O, and the conjugate was isolated by reversed-phase high-performance liquid chromatography (HP-1100, Agilent, Palo Alto, CA, USA) using a linear gradient of water (containing 0.05% trifluoroacetic acid)–acetonitrile (containing 0.08% trifluoroacetic acid). Labeled NT (henceforth "NT-DY647") was lyophilized, dissolved in DMSO, and stored at −20 °C prior to use in a binding assay. The identity of the conjugate was verified by mass spectroscopic analysis.

Labeling of anti-CXCR4 monoclonal antibody

The monoclonal antibody anti-CXCR4 (clone 44708) was labeled with PEG4-DY-647-NHS ester. The reactive dye (4 mg/ml in dimethylformamide) was added to the solution of the antibody (2 mg/ml) in sodium bicarbonate buffer (0.1 M, pH 8.3) and incubated at RT in the dark with gentle agitation for 1 h. Unconjugated dye was separated from the labeled protein by size exclusion chromatography using Zetadex-25 fine resin (emp Biotech, Berlin, Germany) and phosphate-buffered saline (PBS) as eluent. A degree of labeling (DOL) of 1.6 was determined spectrophotometrically using extinction coefficients of 203,000 and 250,000 M^{-1} cm^{-1} for a typical antibody in the IgG format at 280 nm and the dye at 653 nm, respectively. Due to the absorbance of the dye DY-647 at 280 nm, a correction factor of 0.031 suggested by the manufacturer was applied for the calculation of the DOL. The labeled antibody was flash-frozen in liquid nitrogen and stored at −80 °C.

Labeling of alprenolol

Briefly, the allyl moiety of alprenolol was exploited to introduce a cysteamine linker using a thio-ene reaction. The resulting intermediate product (amine) was reacted with Cy5-NHS ester to yield the desired fluorescent conjugate alprenolol-Cy5. Details of the synthesis, purification, and characterization of alprenolol-Cy5 are described in the online supplementary material.

Cell culture and receptor expression

Human embryonic kidney HEK293 cells were cultured in Dulbecco's modified Eagle's medium with high glucose (cat. no. BE12-604F; Lonza, Basel, Switzerland) in the presence of 10% (v/v) fetal calf serum (cat. no. S0115; Biochrom, Berlin, Germany) and 5% CO_2 at 37 °C in a humidified incubator.

Typically, HEK293 cells (5 × 106) were transfected with 8 μg of plasmids encoding GFP-tagged GPCR using the Nanofectin transfection kit (cat. no. Q051-005; PAA, Cölbe, Austria). Transfected cells were investigated microscopically or harvested 24 h after the transfection. Alternatively, the transfected cells were selected using zeocin (cat. no. R25001; Life Technologies) at a concentration of 0.1 mg/ml over a period of several weeks to generate stably

transfected cell lines. During the harvest, the cells were washed twice with PBS, pelleted for 5 min at 1100*g*, and then frozen at −80 °C.

Membrane preparation and receptor solubilization

A cell pellet corresponding to approximately 2 × 107 cells harvested from one 14.5-cm dish was resuspended in 1 ml of ice-cold TBS (50 mM Tris–HCl [pH 7.4] and 150 mM NaCl) supplemented with protease inhibitor cocktail (Complete; Roche, Basel, Switzerland) (henceforth "TBS/PI") and broken by sonication on ice (10 cycles: 15-s probe sonication at 35 W, 50% of the time, 15-s pauses in between) using an Ultrasonic homogenizer SONOPULS HD 2070 (Bandelin, Berlin, Germany). Cell debris was removed by centrifugation for 5 min at 1100 *g* at 4 °C, and the supernatant was centrifuged for 1 h at 21,000 *g* at 4 °C. The resulting pellet containing cellular membranes was then rinsed with 500 μl of TBS/PI and resuspended in 500 μl of TBS/PI by using a Dounce homogenizer (tight pestle). This suspension is denoted as "membrane preparation." Protein content in the membrane preparation was determined using a BCA (bicinchoninic acid) Protein Assay Kit (Thermo Scientific, Rockford, IL, USA), and aliquots of the membrane preparation were flash-frozen in liquid N_2 for long-term storage at −80 °C.

For GPCR solubilization, the membrane preparation was diluted with TBS/PI to a concentration of 1 mg/ml (total membrane protein), and 20-fold concentrated single detergent or detergent mixture was added. For NTR1 and CXCR4, the highest activity was obtained with the mixture of detergents DDM (*n*-dodecyl β-D-maltoside)/CHAPS/CHS (cholesteryl hemisuccinate) at their final concentrations of 0.25/0.5/0.1% (w/v), respectively. For ADRB2, the best results were obtained with DDM at a final concentration of 0.5% (w/v). The membrane preparation was solubilized for 1 h at 4 °C with end-over-end rotation. Insoluble material was pelleted by centrifugation typically for 1 h at 100,000 *g* at 4 °C. Supernatant containing solubilized GPCRs was used in ligand binding assays, which were carried out at RT unless stated otherwise.

Live cell imaging/confocal microscopy

Confocal laser scanning microscopy was conducted on an LSM510 confocal microscope connected to an Axiovert 200M equipped with a C-Apochromat 40 × water immersion objective, NA 1.2 (Carl Zeiss, Jena, Germany), in multitrack mode. Fluorophores AlexaFluor 647 (AF647), Cy5, and DY-647 were excited using a 633-nm helium–neon laser, whereas the 488-nm laser line of an argon–ion laser was employed to excite the enhanced GFP.

The emitted fluorescent light was directed over a main dichroic beam splitter HFT UV/488/543/633 and then separated by a series of secondary dichroic beam splitters; light at longer wavelengths that passed through the NFT 635 VIS dichroic beam splitter and a 650LP longpass filter was detected by the photomultiplier tube (PMT) for the red (Cy5) channel, whereas light at shorter wavelengths that was redirected at the NFT 635 VIS and NFT 545 dichroic beam splitters and passed through a BP505-550 bandpass filter was collected at the PMT detector for the green (GFP) channel.

Fluorescence cross-correlation spectroscopy

FCCS measurements with samples at equilibrium (typically with a volume of 20 μl) were performed with a ConfoCor2 FCS unit connected to an Axiovert 200M equipped with a C-Apochromat 40xwater immersion lens, NA 1.2 (Carl Zeiss), whereas FCCS data for binding kinetics were acquired on an Insight plate reader (Evotec Technologies, Hamburg, Germany) fitted with a U-Apo300 40xwater immersion lens, NA 1.15 (Olympus, Germany). Both systems used a 633-nm helium–neon laser for excitation of Cy5, AF647, and DY647 dyes and the 488-nm laser line of an argon–ion laser to excite the enhanced GFP. At the ConfoCor2 instrument, the emitted fluorescent light was directed over an HFT 488/633 and an NFT 610 beam splitter to the avalanche photodiode (APD). Fluorescence in the green (GFP) channel was detected using a BP500-550 bandpass filter, whereas fluorescence in the red (Cy5) channel was detected using an LP650 longpass filter. At the Insight instrument, the emitted light was split into two APD channels equipped with an HQ 535/50 bandpass filter for green fluorescence and a 670DF40 bandpass filter for red fluorescence. The fitting of the autocorrelation functions and data analysis were carried out either in the ConfoCor2 software or with FCS + plus (Evotec Technologies software). Data acquisition for samples in equilibrium typically took 20–60 s per sample. The kinetics was monitored by FCCS over the course of 20–60 min, during which the single measurements were taken for 5–20 s depending on the rate of the complex formation.

Equilibrium binding models

To determine the total active receptor level (R_T) of a solubilized GPCR and the equilibrium dissociation constant (K_D) of its respective fluorescent probe (L) from the saturation binding FCCS data, we used a two-state single-site binding model. Data from binding assays with NTR1, ADRB2, or CXCR4 for which labeled small molecules or peptides were available were fitted by using Eq. (1) in order to obtain best estimates of R_T and K_D:

$$C = \frac{R_T L_F}{K_D + L_F} = \frac{R_T L_T p\left(t_f\right)}{K_D + L_T p\left(t_f\right)}, \tag{1}$$

where C is concentration of receptor–fluorescent probe complexes calculated from the number of cross-correlating particles. L_T and L_F were derived from autocorrelation function for Cy5 signal and relate to concentrations of total and free labeled fluorescent probe, respectively. $p(t_f)$ is the population of free (i.e., fast-moving) fluorescent probe. t_f is diffusion time of free fluorescent probe and was obtained from one-component fit of Cy5 signal acquired in the presence of a competitor in a large molar excess. $p(t_f)$ value was obtained from two-component fit of Cy5 signal acquired for a fluorescent probe applying autocorrelation function with a fixed diffusion time t_f.

FCCS data from saturation binding assays where a labeled specific antibody in IgG format was used as a surrogate fluorescent probe for CXCR4 (IgG is a relatively large molecule with a diffusion time similar to that of the solubilized receptor) were fitted by applying Eq. (2), which does not require prior determination of $p(t_f)$ or L_F:

$$C = \frac{R_T + L_T + K_D - \sqrt{(R_T + L_T + K_D)^2 - 4R_T L_T}}{2}. \tag{2}$$

The advantage of fitting FCCS data from equilibrium saturation binding assays by applying Eq. (1) is that potential off-target binding of the labeled ligand cannot skew the K_D determination.

IC_{50} values were determined from competition binding data by using a previously described four-parameter logistic function (see Eq. (1) in Ref. [24]). The equilibrium dissociation constant for a competitor (inhibition constant K_I) was calculated by using by the Cheng–Prusoff equation [25].

Kinetic model for binding of a fluorescent probe

Standard one binding site model for reversible interaction between free receptor (R_F) and free fluorescent probe (L_F) is defined in Eq. (3), where k_1 (or k_{on}) is the association rate constant and k_2 (or k_{off}) is the dissociation rate constant:

$$R_F + L_F \underset{k_2}{\overset{k_1}{\rightleftharpoons}} C. \tag{3}$$

During kinetic measurements, we routinely applied fluorescent probes at ≥ 10 M excess over R_T and, thus, assumed only negligible changes in concentration of L_F during the binding of fluorescent probe to its cognate receptor ($L_F \approx L_T$). Pseudo first-order reaction rates k_{obs} were determined for a concentration series of a fluorescent probe (L_T) at a constant receptor concentration (R_T) by fitting the concentration of complexes (C) to monoexponential kinetic Eq. (4) adapted from Ref. [26]:

$$C_t = C_{eq}\left(1 - e^{-k_{obs}\,t}\right), \tag{4}$$

where C_{eq} is the concentration of complexes at equilibrium. Rate constants k_1 and k_2 were obtained from the plot of k_{obs} values against the corresponding L_T values applying linear Eq. (5):

$$k_{obs} = L_T\,k_1 + k_2. \tag{5}$$

Kinetic model for binding of unlabeled competitor

The kinetic parameters for an unlabeled competitor (I) were calculated based on the theoretical model developed by Motulsky and Mahan [27]. Following this model, a fluorescent probe with known binding kinetics (i.e., rate constants k_1 and k_2 were determined in preliminary experiments) was co-incubated with a competitor. The competition binding kinetics of the fluorescent probe is dependent on both the concentration and kinetic parameters of the competitor [27]; therefore, the experimentally derived rate of specific ligand binding can be fitted to provide the association and dissociation rates of the unlabeled competitor. In this work, a simple model of competition kinetics was employed, defined by standard Eqs. (3) and (6):

$$R_F + I_F \underset{k_4}{\overset{k_3}{\rightleftharpoons}} RI, \tag{6}$$

where R_F, I_F, and RI are the concentrations of free receptor, free competitor, and the receptor–competitor complex, respectively. Assuming that only a small fraction (<10%) of fluorescent probe and competitor binds to receptors (i.e., $L_F \approx L_T$ and $I_F \approx I_T$), the following set of equations (Eqs. (7)–(12)) can be derived from standard Eqs. (3) and (6) in order to fit R_T and rate constants k_3 and k_4:

$$K_A = k_1 L_T \cdot 10^{-9} + k_2 \tag{7}$$

$$K_B = k_3 I_T \cdot 10^{-9} + k_4 \tag{8}$$

$$S = \sqrt{(K_A - K_B)^2 + 4k_1k_3L_TI_T \cdot 10^{-18}} \tag{9}$$

$$K_F = 0.5\,(K_A + K_B + S) \tag{10}$$

$$K_S = 0.5\,(K_A + K_B - S) \tag{11}$$

$$C_t = R_T \frac{k_1 L_T \cdot 10^{-9}}{K_F - K_S}\left[\frac{k_4(K_F - K_S)}{K_F K_S} + \frac{(k_4 - K_F)}{K_F}e^{-K_F t} - \frac{(k_4 - K_S)}{K_S}e^{-K_S t}\right]. \tag{12}$$

Concentrations of L_T, I_T, and R_T are in units of nM, k_1 is in units of M^{-1} min^{-1}, and k_2 is in units of min^{-1}. Association rate constant k_3 (M^{-1} min^{-1}) and dissociation rate constant k_4 (min^{-1}) for the competitor were calculated by fitting the data from the competition kinetic experiments, C_t versus time t, by applying Eqs. (7)–(12). Furthermore, prior to nonlinear regression, obvious outliers were removed from datasets.

Results

Preparation of fluorescent probes and their characterization by live cell imaging

To evaluate a general applicability of FCCS for the analysis of GPCR–ligand interactions, we decided to test fluorescently labeled representative examples of four distinct probes: (i) a small organic molecule (antagonist alprenolol), (ii) a short peptide (endogenous agonist NT), (iii) a cytokine (endogenous agonist SDF1α), and (iv) a monoclonal antibody in the IgG format (antagonistic anti-CXCR4 antibody). The latter example (a blocking antibody) can be used as a surrogate probe in the case where endogenous ligands are unknown (orphan GPCRs) or where known ligands do not possess a suitable reactive group for coupling to a fluorescent dye. The GPCR targets of the selected compounds are pharmaceutically relevant GPCRs of the class A family: NT is an agonist of neurotensin receptor type 1 involved in hyperthermia, pain, schizophrenia, Parkinson disease, and cancer; SDF1α and the anti-CXCR4 monoclonal antibody recognize an active form of human C-X-C chemokine receptor type 4, an extensively validated drug target in cancer and AIDS; and alprenolol is an antagonist of β2-adrenergic receptor, which plays a crucial role in hypertension and cardiac arrhythmia.

The selected probes were labeled with Cy5, AF647, or DY-647, all of which are far-red fluorophores emitting in the spectral range above 650 nm. The fluorescent conjugates are referred to as “fluorescent probes” in the text below.

The selected GPCRs were recombinantly expressed with the C-terminal GFP fusion in stably transfected HEK293 cells. By choosing the enhanced GFP as a fluorescent tag for GPCRs, we ensured a minimal spectral overlap with fluorescence emission from the labeled probes. In each case, the GFP signal was present mainly in the plasma membrane, and only a minor population of the receptor fusions resided in internal cellular compartments (endoplasmic reticulum/Golgi apparatus/endosomes) (Fig. 1; see also Fig. S1 in supplementary material). In general, GPCR localization in the plasma membrane correlates well with a proper GPCR folding, translocation, and activity [28,29].

When we added the fluorescent probes in two-digit nanomolar concentrations into the cell culture medium, we observed a strong overlap between the GFP and Cy5/AF647/DY-647 signals at the plasma membrane, which indicated that both the GFP-tagged receptors and the fluorescent probes are functional. The cell surface staining with the fluorescent probes was highly target specific, and it was completely prevented in the presence of receptor-specific competitors (Fig. 1 and Fig. S1). The fluorescently labeled antagonist alprenolol and the antagonistic anti-CXCR4 MAb remained localized exclusively on the plasma membrane in cells expressing ADRB2 and CXCR4, respectively, even after a 60-min incubation of the cells at RT (Fig. S1A and S1B). In contrast, the DY-647-labeled

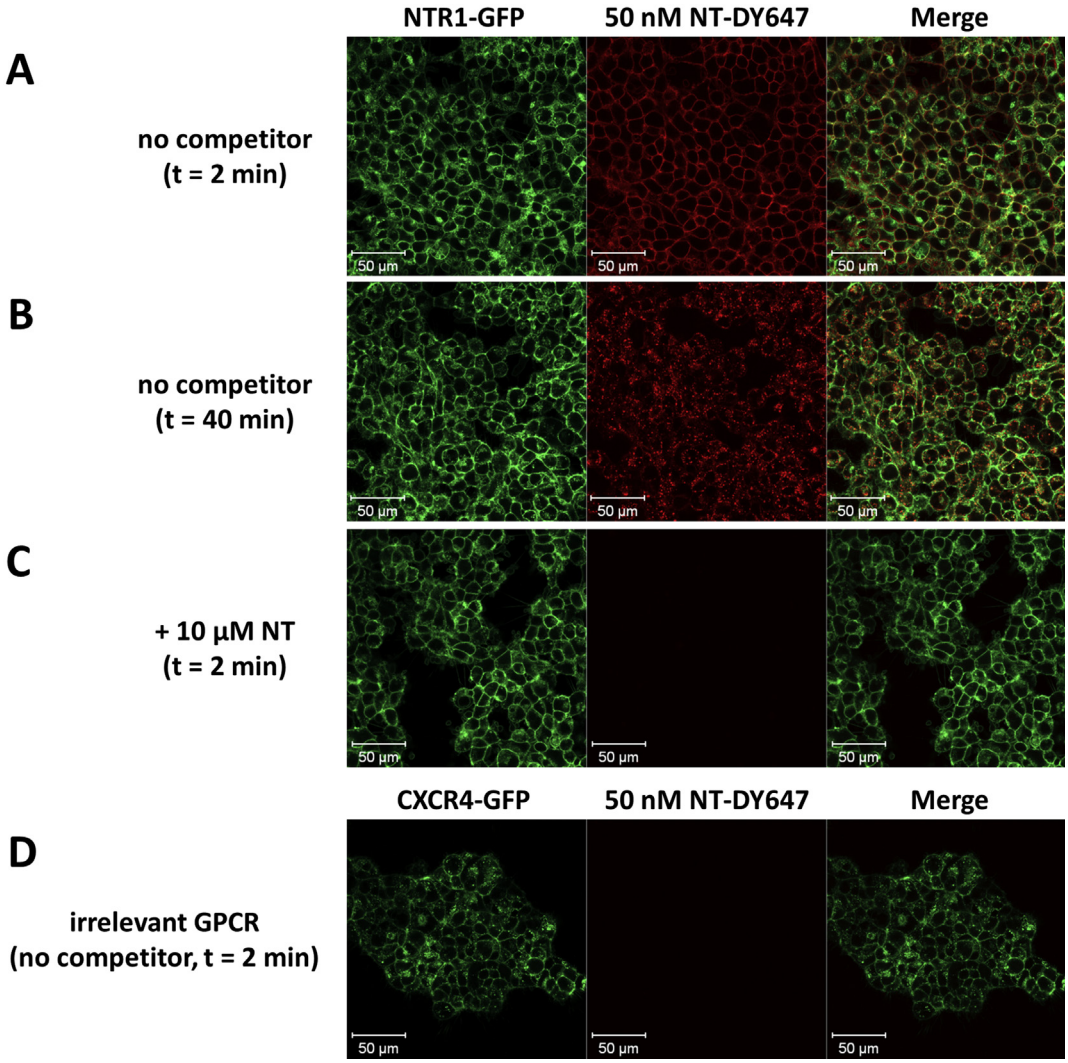

Fig.1. Live cell imaging of NTR1-GFP stably expressed in HEK293 cells and binding of NT-DY647. Images of the NTR1-GFP fusion (green, left panel), mainly localized in the plasma membrane, and the fluorescent probe NT-DY647 (red, middle panel) were obtained by confocal microscopy. Representative images are shown. (A) Co-localization of both NTR1-GFP and NT-DY647 (yellow, right panel) on the cell surface were observed at 2 min following the addition of the fluorescent probe. (B) After 40 min incubation of NT-DY647, NTR1-GFP was partially internalized as well as the fluorescent probe. (C) HEK293 cells expressing NTR1-GFP were incubated with NT-DY647 in the presence of 10 µM unlabeled NT. No NT-DY647 binding was observed. (D) HEK293 cells expressing an irrelevant GPCR-GFP fusion (CXCR4-GFP) were incubated with NT-DY647. No co-localization was observed.

agonist NT was rapidly internalized into the NTR1-expressing cells within 10–20 min under identical conditions (Fig. 1). We also observed internalization of the labeled SDF1α into HEK293 cells expressing CXCR4 (Fig. S1C); however, this process was not as rapid and complete as in the case of the labeled NT internalized into the cells expressing NTR1. Internalization of receptor–ligand complexes is a common event observed on agonist binding to its cognate GPCR [3]. We inferred from these data that the three GFP-fused GPCR targets and their cognate fluorescent probes are functional and hence can be applied in FCCS.

Solubilization of GPCRs in a functional form

FCCS allows the detection and real-time monitoring of intermolecular interactions directly in living cells, in crude cell lysates, or in preparations with purified or partially enriched targets. Although FCS-based detection of ligand–receptor interactions on the plasma membrane of intact cells has been reported for several GPCRs [30–38], this application is technically demanding and time-consuming and is not amenable to high-throughput screening (HTS). However, FCS/FCCS can be run in HTS format with monodisperse solutions containing soluble or solubilized targets. In the case of hydrophobic integral membrane proteins, such as GPCRs, solutions containing native proteins can be prepared on solubilization of whole cells or isolated membranes by using detergents [39].

In initial experiments, we set out to solubilize NTR1 in a functional form by using DDM/CHAPS/CHS as a detergent mixture that was initially used by Tucker and Grisshammer for the solubilization of NTR1 from *Escherichia coli* membranes [40]. This detergent mixture has also been used successfully by others for the selection of stabilized engineered NTR1 variants [21,41] as well as for the selection of specific NTR1 binders from the DARPin library by using ribosome display [42]. Because it has been reported that wild-type NTR1 is unstable at RT, we tested in parallel mutated variants of human NTR1 that were shown to have substantially higher stability in detergents: single mutants Ala85Leu, Ile252Ala, and Phe353Val and a triple mutant TTM that combines these three single

mutations [22,43]. Indeed, we observed by FCCS that wild-type NTR1 is highly unstable at RT, whereas the mutated NTR1 variant with three mutations A85L/I252A/F353V as well as the single mutant NTR1-A85L exhibited high stability in the solubilized state; although very little ligand binding was observed for the WT receptor at RT, the ability of the two mutants (TTM and A85L) to specifically bind the labeled ligand NT-DY647 at a concentration of 20 nM was minimally affected on incubation in detergent for 1 h at RT. The ligand binding to mutants I252A and F353V was quite low at RT, which is probably due to lower stability of these two single mutants in comparison with the NTR1 variants TTM and A85L (Fig. S2). In Fig. S3A and Table S1 in the supplementary material, we show for solubilized stabilized mutant NTR1-A85L an example of FCCS data transformed using autocorrelation and cross-correlation functions. The data acquired with the labeled ligand and active receptor applied at their approximately stoichiometric concentrations clearly indicate that the binding of NT-DY647 to detergent-solubilized NTR1-A85L is (i) accompanied by a shift in diffusion time of NT-DY647 due to a substantial difference in molecular weight of free and receptor-bound NT-DY647 and (ii) completely inhibited in the presence of large excess of unlabeled NT (10 μM).

We solubilized ADRB2 in the functional form with DDM alone, which was previously applied by Kobilka and coworkers for solubilization, purification, and crystallization of this receptor [44,45]. Similarly as for NTR1-A85L, the FCCS data clearly indicate that the binding of the fluorescent probe (alprenolol-Cy5) to DDM-solubilized ADRB2 was (i) accompanied by a shift in diffusion time of labeled alprenolol due to a substantial difference in molecular weight of free and receptor-bound alprenolol-Cy5 and (ii) completely inhibited in the presence of 10 μM unlabeled alprenolol (Fig. S3B and Table S1).

The FCS analysis of diffusion time of the solubilized receptor indicated monodispersity for solubilized wild-type ADRB2 as well as for the solubilized stabilized NTR1 variant A85L; only a single population with diffusion time of approximately 200–250 μs (derived from one-component fit; Table S1) was identified for these two solubilized GPCRs.

CXCR4 was successfully solubilized with the detergent mixture DDM/CHAPS/CHS. Specific interaction with solubilized CXCR4 was clearly detected by FCCS for both fluorescent probes: SDF1α -AF647 and anti-CXCR4 MAb-DY647. In Fig. S3C and S3D, we show examples of FCCS data transformed using autocorrelation and cross-correlation functions for the two fluorescent probes of CXCR4; the binding of the fluorescent probes to detergent-solubilized CXCR4 was accompanied by a clear shift in diffusion time of the fluorescent probes (Fig. S3C and S3D and Table S1). Intriguingly, binding of anti-CXCR4 MAb-DY647 to CXCR4 could not be completely inhibited in the presence of 10 μM unlabeled small molecule IT1t (Fig. S3D). The residual binding of anti-CXCR4 MAb-DY647 seen in the presence of competitor was most likely due to a partially non-overlapping binding site of anti-CXCR4 MAb and IT1t given that no cross-correlation was detected on incubation of anti-CXCR4 MAb-DY647 with an irrelevant GFP-fused GPCR solubilized under the same conditions as CXCR4 (Fig. S3D).

The FCS analysis of diffusion time of solubilized CXCR4 indicated two receptor populations: a major one (~80%) with diffusion time t_1 of approximately 280 μs and a minor one (~20%) of receptor aggregates with an approximately 5-fold slower diffusion time t_2 (diffusion times t_1 and t_2 were derived from two-component fit; Table S1).

Besides diffusion time, FCS analysis also provides information about concentration (particle count) and the molecular brightness of the fluorophores/fluorescently labeled molecules [46]. Molecular brightness constitutes the fractional contribution of each particle to the total fluorescence and can be used to study oligomerization or receptor–ligand stoichiometry [32,47]. Analyzing the molecular brightness and particle count for the tested fluorescent probes alprenolol-Cy5, NT-DY647, and SDF1α-AF647 in the presence of their cognate solubilized GPCRs, the FCS data did not reveal any difference in these parameters between the receptor–ligand binding reactions carried out in the presence or absence of competitors (data not shown; experimental conditions are described in the legend of Table S1), indicating the stoichiometry of the receptor–ligand binding 1:1 where we refer to a receptor molecule as a solubilized GPCR-GFP fusion in a detergent micelle.

The analysis of the molecular brightness and particle count for the fluorescently labeled anti-CXCR4 MAb tested under the experimental conditions described in the legend of Table S1 revealed a decrease of approximately 30% in the particle count and an increase of approximately 30% in molecular brightness of anti-CXCR4 MAb-DY647 in the presence of solubilized CXCR4 (data not shown), which can be reconciled with the 2:1 binding stoichiometry for solubilized CXCR4 bound to an anti-CXCR4 bivalent monoclonal antibody (IgG format) applied in a sub-stoichiometric amount.

Determination of equilibrium binding constants for solubilized GPCRs

Following demonstration of specificity of ligand binding and the optimization of solubilization conditions, we determined ligand binding affinities for the selected GPCRs. Because wild-type NTR1 was unstable at RT, we conducted further ligand binding experiments with NTR1-WT at 4 °C. The stabilized NTR1 variants TTM and A85L, as well as wild-type ADRB2 and CXCR4, were incubated with tested compounds at RT.

First, we performed saturation binding assays to determine the equilibrium dissociation constants (K_D) for the interaction between the solubilized GPCRs and their fluorescent probes. Data from the equilibrium saturation binding assays are shown in Fig. 2, and calculated K_D values are summarized in Table 1. Intriguingly, the determined affinity of NTR1 variants for the labeled NT increased in rank: WT < A85L < TTM, which correlates with the observed differences in the stability of solubilized NTR1 variants (see Fig. S2 in supplementary material).

In the next step, we determined in competition binding assays inhibition constants (K_I) for several commercially available ligands of ADRB2, NTR1, and CXCR4. Noteworthy, in our competition binding assays we worked with solubilized receptors diluted to the concentration of approximately 3–5 nM and with fluorescent probes at concentrations slightly above their K_D values. We ensured by these measures that the depletion of fluorescent probes due to their binding to a specific target was below 10% in order to fulfill the criteria of the Cheng–Prusoff equation ($L_F \approx L_T$).

The K_I values determined for a series of unlabeled ADBR2 ligands alprenolol, propranolol, CGP 12177, and ICI 118551 ranged from 6 to 16 nM, whereas the reported K_I values determined by other methods for these compounds were up to 1 log lower (Table 2 and Fig. 3). The K_I values for agonist norepinephrine (~30 μM) was in very good agreement with previously published K_I values determined by other techniques (Table 2 and Fig. 3).

The K_I values obtained with solubilized NTR1-WT or NTR1-A85L for NTR1 ligands matched well with previously published K_I values determined by other techniques (Table 3). Intriguingly, compared with the wild-type NTR1, the stabilized triple mutant NTR1-TTM showed approximately 17-fold weaker affinity for antagonist SR 48692, although the affinities determined for agonist NT and antagonist SR 142948 were similar between the two receptor variants (Table 3). This finding is consistent with a previously published study where a single mutation of Phe358 to Ala in rat NTR1

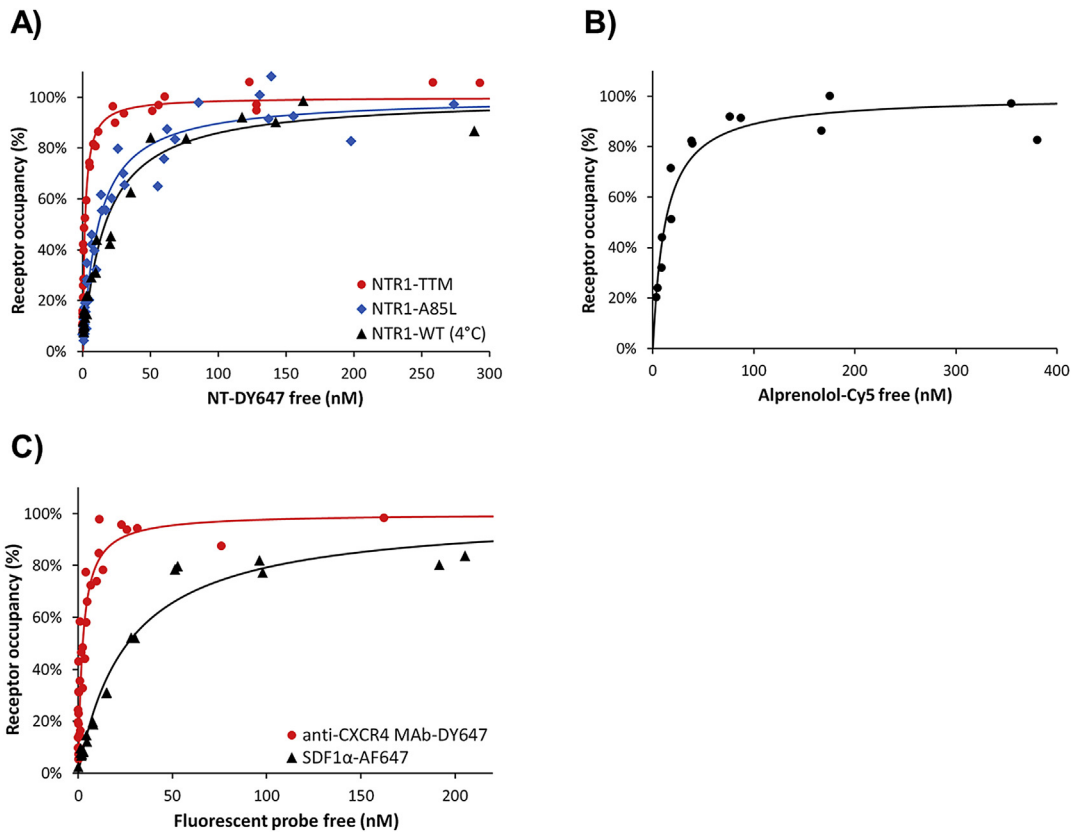

Fig.2. Equilibrium saturation binding assays with solubilized GPCRs and fluorescent probes. Membranes from HEK293 cells expressing a GPCR-GFP fusion were isolated and solubilized as described in Materials and Methods. During the binding assays, solubilized receptors were incubated for 1–2 h at RT (or at 4 °C in the case of NTR1-WT) with fluorescent probes at various concentrations: (A) NT-DY647 was used for NTR1 variants; (B) alprenolol-Cy5 was used for wild-type ADRB2; (C) SDF1α-AF647 and anti-CXCR4 MAb-DY647 were used for wild-type CXCR4. Transformed FCCS data (concentration of receptor–ligand complexes (*C*) were fitted with Eq. (1) for NTR1 variants and for ADRB2 or with Eq. (2) for CXCR4.

(corresponding to the position F353 in human NTR1; mutation F353V is present in the TTM triple mutant) was reported to result in approximately 5-fold lower affinity of the receptor for SR 48692 [48].

Both CXCR4-specific fluorescent probes (SDF1α-DY647 and the anti-CXCR4 MAb-DY647) proved to be valuable; binding assays using these fluorescent probes yielded for three different competitors very similar K_I values, which are also close to those reported in the literature (Table 4).

Overall, when we compare our FCCS-based K_I values with data from radioligand binding assays reported in the literature, we find good agreement with previously published data for all three tested GPCRs (Tables 2–4).

Table 1
Determination of K_D values in equilibrium binding assays by FCCS for selected solubilized GPCRs and various fluorescent probes.

GPCR	Fluorescent probe[a]	K_D[b] (nM)	T[c]
NTR1-WT	NT-DY647	17 ± 3	4 °C
NTR1-A85L	NT-DY647	12 ± 2	RT
NTR1-TTM	NT-DY647	1.7 ± 0.1	RT
ADRB2	Alprenolol-Cy5	13 ± 2	RT
CXCR4	SDF1α-AF647	26.2 ± 0.6	RT
CXCR4	anti-CXCR4 MAb-DY647	2.7 ± 0.8[d]	RT

[a] Preparation of fluorescent probes is described in Materials and methods.
[b] K_D values are expressed as means ± standard errors.
[c] T is temperature at which the binding assay was performed.
[d] Functional affinity (avidity) [63] considering the multivalent nature of the fluorescent probe; labeled monovalent antibody in the IgG format.

Determination of binding kinetics using FCCS

Compounds with the same affinity (K_D) but different association and dissociation rates can have a very different biological activity profile. Drug target residence time, which is the reciprocal of the dissociation rate constant ($1/k_{off}$), has been found to have a considerable impact on target selectivity and duration of effect because typically a drug is efficacious only as long as it binds to, and modulates the action of, its physiological target(s) [49–52].

Table 2
Determination of K_I values in equilibrium binding assays by FCCS for solubilized human ADRB2 by using alprenolol-Cy5 as fluorescent probe.

Competitor	FCCS[a]	Literature
(rac) Alprenolol	10 ± 4 nM	2–6 nM[b]
(rac) Propranolol	16 ± 7 nM	0.6–1.1 nM[c]
(−)-Norepinephrine	33 ± 2 μM	4–97 μM[d]
CGP 12177	6 ± 2 nM	0.4 nM[e]
(R-) ICI 118551	12 ± 6 nM	0.6 nM[e]/3–4 nM[f]

[a] K_I values are expressed as means ± standard errors.
[b] Determined in radioligand binding assays with solubilized ADRB2 [64,65].
[c] Determined in radioligand binding assays with membrane preparations or whole cells [66–68].
[d] Determined in radioligand binding assays with membrane preparations [67,69,70].
[e] Determined in radioligand binding assays with membrane preparations or whole cells [66,68].
[f] Determined in radioligand binding assays with ADRB2 solubilized from hamster or rat lung [71].

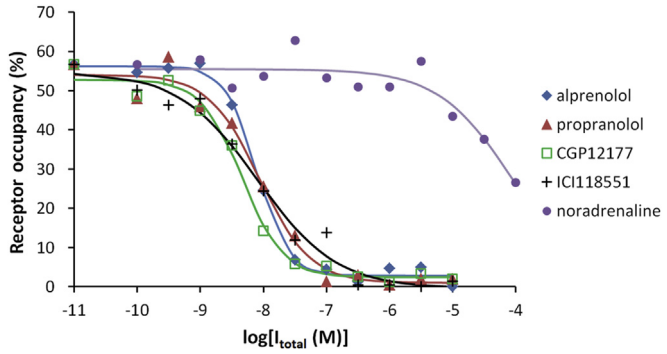

Fig.3. Equilibrium inhibition binding assay with solubilized ADRB2. Membranes from HEK293 cells stably expressing ADRB2-GFP fusion were isolated and solubilized as described in Materials and Methods. The solubilized receptor and fluorescent probe alprenolol-Cy5 applied at a constant concentration and unlabeled competitors applied at various concentrations were incubated together at RT for 1–2 h. Data from a representative experiment where [alprenolol-Cy5] = 20 nM are shown. Transformed FCCS data (concentration of receptor–ligand complexes *C*) were fitted by using a four-parameter logistic function as indicated in Materials and Methods.

For this reason, we also opted to characterize kinetics of the receptor–ligand interaction for a few selected fluorescent probes as well as for unlabeled competitors. As examples of GPCR targets, we chose NTR1 and CXCR4 mainly because kinetic data acquired in homogeneous binding assays had been reported for these two receptors [53–55]. We applied the active solubilized receptors at a concentration of approximately 2 nM and adjusted concentrations of fluorescent probes and unlabeled competitors to levels that exceed the concentration of the receptor by a factor of ≥10. In this way, we ensured that during the whole course of kinetic measurements, the depletion of fluorescent probes or unlabeled competitors due to their binding to a specific target was below 10% (i.e., $L_F \approx L_T$ and $I_F \approx I_T$) in order to comply with the assumptions of the kinetic models implemented in this study. First, we determined kinetic parameters k_{obs}, k_{on}, and k_{off} for the fluorescent probes NT-DY647 and SDF1α-AF647 using samples with solubilized NTR1-A85L and CXCR4, respectively (Fig. 4 and Table 5) as described in detail in Materials and Methods. Fig. 4A and B show examples of kinetic traces for the two fluorescent probes analyzed at various concentrations (L_T values) for their binding to their cognate receptors. The association rate of a fluorescent probe (k_{on}) was calculated as the slope of a line that represents a plot of k_{obs} versus the corresponding L_T, whereas the dissociation rate (k_{off}) is determined by the *y*-intercept of the line (Fig. 4C and Table 5).

In the next step, we determined k_{on} and k_{off} values for representative unlabeled competitors known to interact with NTR1 or CXCR4. As shown in Table 6, the resulting K_I values match quite well with the K_I values obtained from the equilibrium competition binding assays. In Fig. 5, we show examples of time-resolved binding of fluorescent probes to solubilized cognate receptors in the absence or presence of different unlabeled competitors. The data could be fitted in concordance with the kinetic model described in Materials and Methods (Eqs. (6)–(12)) and theory elaborated elsewhere [27]. Kinetic traces of unlabeled NT and SR 48692 (ligands of NTR1) (Fig. 5A) are typical for a competitor that has a slower dissociation than the corresponding fluorescent probe (here NT-DY647; $k_4 < k_2$), whereas the kinetic traces of unlabeled IT1t and SDF1α (ligands of CXCR4) (Fig. 5B) are typical for a competitor that has a faster dissociation than a corresponding fluorescent probe (here SDF1α-AF647; $k_4 > k_2$) [27].

Our kinetic parameters and resulting K_I values are also in good agreement with data published by other groups that used surface plasmon resonance (SPR) for time-resolved affinity determination [53,54]. A discrepancy in the dissociation rate constant for unlabeled SDF1α determined by FCCS (k_{off}: 0.23 ± 0.03 min^{-1}) and SPR (k_{off}: 4.8–30 min^{-1}) might be due to numerous differences in the experimental setup (immobilization of CXCR4 in SPR vs. freely diffusing assay components in FCCS and/or additives used in the particular SPR setups such as $MgCl_2$, $CaCl_2$, and extra lipids) [54].

Intriguingly, we have noticed for both probes NT and SDF1α an approximately 1-log difference in affinity for their cognate GPCR targets when comparing K_D and K_I values of the labeled and unlabeled forms of a probe, respectively. Although the dissociation rate ($k_{off} = 1/\text{residence time}$) did not vary substantially between the two

Table 3
Determination of K_I values in equilibrium binding assays by FCCS for solubilized human NTR1 variants by using NT-DY647 as fluorescent probe.

Competitor	FCCS (nM)[a]			Literature (nM)
	WT	A85L	TTM	WT
NT	2 ± 0.6	1.2 ± 0.2	0.6 ± 0.04	0.2–5[b]
SR 142948	0.9 ± 0.2	0.8 ± 0.2	1.9 ± 0.3	0.3–1[c]
SR 48692	8 ± 5	8 ± 3	130 ± 30	4[d]

[a] K_I values are expressed as means ± standard errors.
[b] Determined in radioligand binding assays with membrane preparations or whole cells [23,72,73].
[c] Determined in radioligand binding assays with membrane preparations [74].
[d] Determined in radioligand binding assays with membrane preparations [72].

Table 4
Determination of K_I values in equilibrium binding assays by FCCS for human CXCR4.

Competitor	FCCS (nM)[a]		Literature (nM)
	Probe: SDF1α-AF647	Probe: MAb[b]	
SDF1α	9 ± 1	4 ± 2	3.6–85[c]
IT1t	2.4 ± 0.9	5 ± 2	7.9–22.5[d]
TC14012	6 ± 2	14 ± 2	2.9[e]

[a] K_I values are expressed as means ± standard errors.
[b] Anti-CXCR4 MAb-DY647.
[c] Determined in radioligand binding assays with whole cells or membrane preparations [75–79].
[d] Determined in radioligand binding assays with membrane preparations [80,81].
[e] Determined in radioligand binding assays with whole cells [82]. The K_I value was calculated from the IC_{50} value using the Cheng–Prusoff equation applying the K_D value of [^{125}I]SDF1α = 7.9 nM [75].

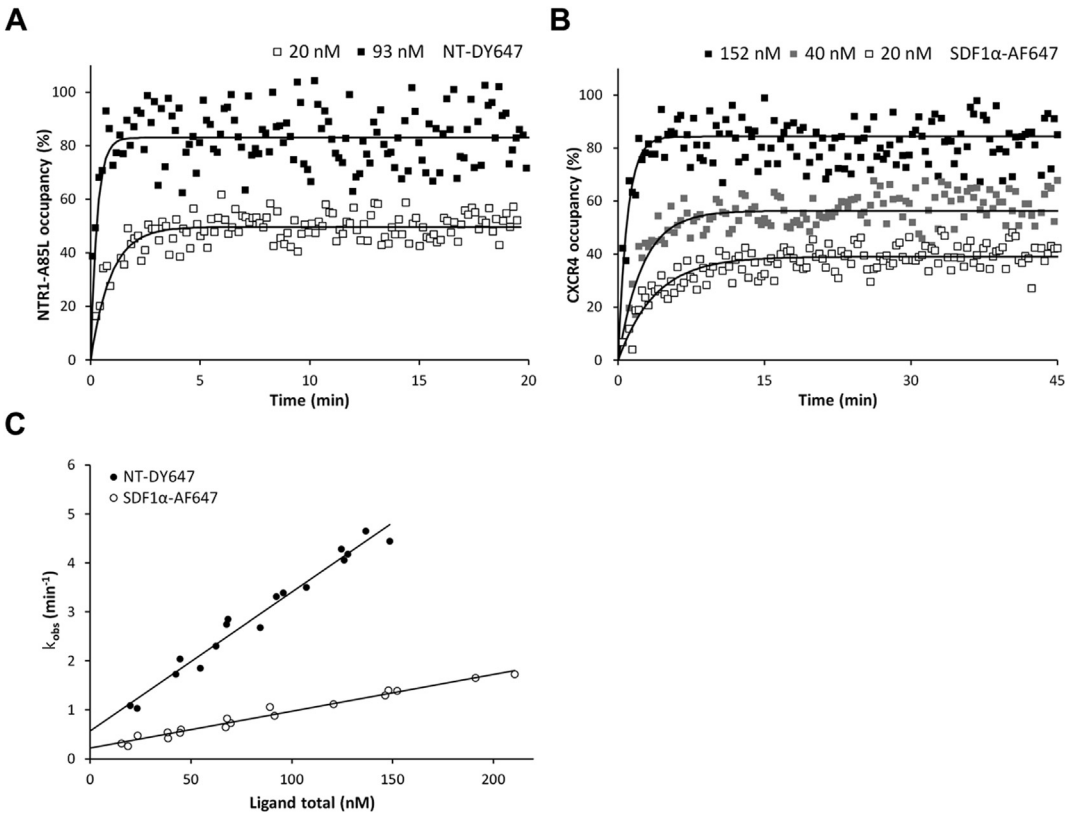

Fig.4. Kinetics studies of both fluorescent probes NT-DY647 and SDF1α-AF647 by FCCS. (A) Representative time-resolved measurements of the interaction between 1.75 nM solubilized NTR1-A85L-GFP and the two indicated concentrations of NT-DY647. Data points are experimental values of complexes measured for 8 s. The solid lines represent the best fitted curves according to Eq. (4) and yielding reaction rates k_{obs} of 1.1 and 3.4 min^{-1} for 20 and 93 nM DY-647, respectively. (B) Representative time-resolved measurements of the interaction between 2 nM solubilized CXCR4 and the three indicated concentrations of SDF1α-AF647. Data points are experimental values of complexes measured for 18 s. The fits yielded k_{obs} of 0.3, 0.4, and 1.3 min^{-1} for 20, 40, and 93 nM SDF1α-AF647, respectively. (C) The k_{obs} values determined in three independent experiments were plotted versus the different concentrations of fluorescent probes used. The solid line represents the best linear regression, and k_{on} and k_{off} of the fluorescent probes were estimated from the slope and *y*-intercept, respectively. k_{on} and k_{off} values of NT-DY647 and SDF1α-AF647 are summarized in Table 5.

Table 5
k_{on} and k_{off} values determined for various fluorescent probes in time-resolved FCCS-based binding assays.

GPCR	Probe	k_{on} (nM^{-1} min^{-1})	k_{off} (min^{-1})	K_D (Kinetics, nM)	K_D (Equilibrium, nM)
NTR1-A85L	NT-DY647	0.0287 ± 0.0005	0.6 ± 0.1	20 ± 4	12 ± 2
CXCR4	SDF1α-AF647	0.0076 ± 0.0003	0.22 ± 0.05	29 ± 8	26.2 ± 0.6

Table 6
k_{on} and k_{off} values for unlabeled competitors of NTR1 or CXCR4 determined in time-resolved FCCS-based binding assays.

GPCR	Competitor	k_{on} (nM^{-1} min^{-1})	k_{off} (min^{-1})	K_I (Kinetics, nM)	K_I (Equilibrium, nM)
NTR1-A85L[a]	NT	0.19 ± 0.02	0.26 ± 0.02	1.5 ± 0.1	1.2 ± 0.2
	SR 142948	0.16 ± 0.03	0.19 ± 0.02	1.3 ± 0.1	0.8 ± 0.2
	SR 48692	0.020 ± 0.003	0.20 ± 0.02	11 ± 1	8 ± 3
CXCR4[b]	SDF1α	0.10 ± 0.02	0.23 ± 0.03	2.7 ± 0.4	9 ± 1
	IT1t	0.14 ± 0.02	0.78 ± 0.2	6 ± 1	2.4 ± 0.9

Note. All values are expressed as means ± standard errors. The binding assay was performed at room temperature. The data were generated from competition binding assays at concentrations of competitors: 20–50 nM for NTR1 or 10–20 nM for CXCR4.

[a] NTR1-A85L kinetics measurements were performed using NT-DY647 as fluorescent probe.

[b] CXCR4 kinetics measurements were performed using SDF1α-AF647 as fluorescent probe.

forms of the same probe (Tables 5 and 6), there were considerable differences in the association rate (k_{on}) related to the increase in size on the labeling of a probe with a fluorophore (Tables 5 and 6). The increase in size can result in a slower diffusion of the probe through the receptor crevice and hence can hinder the docking of probe molecules within the binding site in the receptor. A longer time needed for binding of the target is typically reflected in lower k_{on} values.

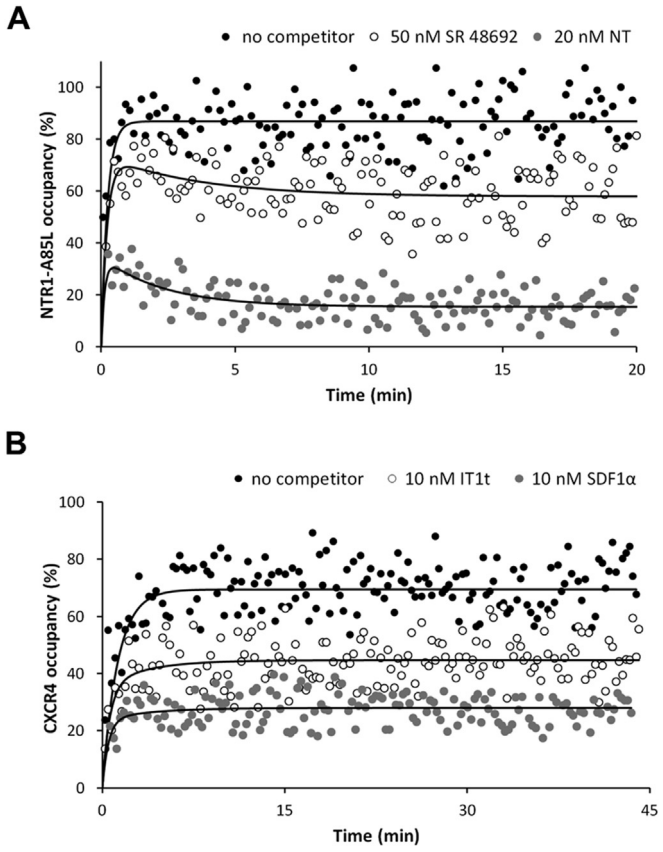

Fig.5. Competitive kinetics with NTR1 and CXCR4 competitors. (A) A representative example of time-resolved measurements of the interaction between approximately 2 nM solubilized NTR1-A85L-GFP and 113 nM NT-DY647 in the absence or presence of 20 nM NT and 50 nM SR 48692. Data points are experimental values of complexes measured for 8 s. (B) Representative time-resolved measurements of the interaction between approximately 1 nM solubilized CXCR4-GFP and 68 nM SDF1α-AF647 in the absence or presence of 10 nM IT1t and SDF1α. Data points are experimental values of complexes measured for 16 s. The solid lines represent the best fitted curves according to Eq. (12) yielding k_{on} and k_{off} values for both unlabeled competitors. k_{on} and k_{off} values of the different competitors tested are summarized in Table 6.

Discussion

In our current study, we have demonstrated on three pharmacologically distinct G protein-coupled receptors (human NTR1, ADRB2, and CXCR4) that fluorescence cross-correlation spectroscopy can be reliably applied for characterization of direct ligand–GPCR interaction in a high-throughput screening mode as well as for determination of kinetic parameters (k_{on} and k_{off} values related to the onset of the compound's effect and residence time on a therapeutic target) for binding of labeled compounds as well as unlabeled compounds. We also showed that almost any molecule within a very broad range of sizes can be used as a probe (e.g., a small molecule, a small or large peptide, or an antibody in IgG format).

In previously published reports, FCS/FCCS has been applied mainly to native nonsolubilized GPCRs in intact cells (in vivo FCS; reviewed elsewhere [31,37]). These measurements are technically tedious, time-consuming, and not straightforward for numerous reasons: (i) focus of the laser beam needs to be stably positioned during the signal acquisition to the upper membrane of the living and therefore motile cells; (ii) a GPCR of interest is often not uniformly distributed in the plasma membrane but rather localizes in membrane microdomains (lipid rafts), making the accurate quantification of receptor complexes demanding; and (iii) the target can undergo endocytotic internalization during the course of the binding assay and therefore obscure the determination of receptor–ligand complexes in equilibrium [30], thereby preventing automation and high-throughput testing of numerous competitors at a wide range of concentrations. Cramb and coworkers published an FCCS-based method for affinity determination by using a model GPCR (μ opioid receptor) embedded in native membranes within vesicles termed "nanopatches." Although the affinity determined in their studies resembled values obtained from radioligand binding assays, the FCCS carried out in the presence of vesicles of poorly defined and very heterogeneous sizes with hundreds of receptor copies/vesicles clearly suffered from sample heterogeneity and required the use of alternative models for "pseudo" K_D determination based on the Hill equation for multiligand binding [56,57].

What are major advantages of FCCS over the other techniques for affinity determination? Many alternative methods have some unique superior features, for instance, extremely high sensitivity and broad dynamic range of radioligand binding assays. However, all alternative techniques have, besides their advantages, also their limitations and weaknesses (extensively reviewed elsewhere [4,55,58]). The presented FCCS-based assay for GPCRs performed in the homogeneous format combines several important features that an assay for affinity determination and kinetics should definitely possess: (i) a technically easy and straightforward procedure (no need for receptor overexpression, purification, or reconstitution in any artificial membranes, nanopatches, or vesicles), (ii) high reproducibility, (iii) good sensitivity and relatively broad linear range (K_I values ranging from subnanomolar to millimolar concentrations can be reliably determined for all kinds of unlabeled competitors regardless of their molecular size), (iv) suitability for automation and high throughput (the assay does not require any washing step and is routinely performed in a 384-well format, and sufficiently robust measurements can be performed in just 5–10 s/data point), (v) relatively versatile design of fluorescent probes (no distance constraints are imposed on a linker between probe and fluorophore and no size limit on a probe as long as it can specifically recognize its target), and (vi) high content information (e.g., about fractions of free/bound ligand and diffusion time/relative molecular size of all fluorescently labeled components during the whole course of binding reaction). Another advantage of using FCCS, in comparison with radioligand binding assays, is the possibility of acquiring data for the whole time course during kinetic measurements continuously from a single well, hence providing substantially better time resolution and saving material.

Our high-throughput FCCS setup involves receptor solubilization with detergents that can cause inactivation of labile GPCR targets. However, we have shown in an example of the neurotensin receptor variant NTR1-A85L that robust FCCS data can also be obtained for GPCRs that are—as wild-type molecules—very unstable in the solubilized form in detergent. A minimal mutagenesis (a single point mutation in the transmembrane domain 1), which is generally not expected to significantly affect receptor functioning, made NTR1 sufficiently stable for the equilibrium measurements as well as the kinetic measurements at room temperature. Several different protein engineering methods, such as alanine scanning and powerful directed evolution approaches based on fluorescence-activated cell sorting (reviewed elsewhere [59]), have enabled selection of numerous thermostabilized GPCRs that were successfully used, for instance, in protein crystallization/structural biology [60]. Some of these reported mutants with slightly enhanced stability and unaffected ligand binding profile contained as little as one single point mutation [61] and thus are suitable for FCCS-based ligand binding studies with wild-type-like receptor molecules when the wild-type receptor is unstable in detergent.

Although not exemplified in this study, the FCCS-based assay can be used not only for determination of K_I values for compounds directly competing for the orthosteric binding site (here a labeled probe is typically derived from an endogenous agonist acting on a given GPCR) but also for identification and characterization of positive and negative allosteric modulators based on their effect on the binding of orthosteric fluorescent probes [62].

Acknowledgments

We thank Maria Koch and Jonas Bertram for excellent technical assistance, Danial Taherzadeh for assistance with preparation of the algorithm for analysis of the kinetics data, Rainer Deutzmann (Institut für Biochemie, Mikrobiologie, und Genetik, Universität Regensburg, Germany) for mass spectroscopic analysis, Annette Beck-Sickinger (Institut für Biochemie, Universität Leipzig, Germany) for plasmids encoding human CXCR4 and Y2 receptor and for recombinant CXCL12/SDF-1α (Lys22-Met93), Roland Brock (Radboud Institute for Molecular Life Sciences, Radboud University Medical Centre, Nijmegen, The Netherlands) for plasmid encoding human ADRB2 and for valuable discussion, and Stefano Minguzzi and Manal Chatila (Intana Bioscience) for critical reading of the manuscript. The study was supported by the German Federal Ministry of Education and Research (BMBF program "KMU innovativ: Biotechnologie–BioChance," grant 031A239A) and by the European Union Framework 7 Marie Curie Initial Training Network "Sphingolipid Homeostasis: From Basic Biology to Applications" (project 289278).

Appendix A. Supplementary data

Supplementary data related to this article can be found at http://dx.doi.org/10.1016/j.ab.2016.02.017.

References

[1] D. Latek, A. Modzelewska, B. Trzaskowski, K. Palczewski, S. Filipek, G protein-coupled receptors—recent advances, Acta Biochim. Pol. 59 (2012) 515–529.
[2] R. Zhang, X. Xie, Tools for GPCR drug discovery, Acta Pharmacol. Sin. 33 (2012) 372–384.
[3] K. Lundstrom, Present and future approaches to screening of G-protein-coupled receptors, Future Med. Chem. 5 (2013) 523–538.
[4] L. Chen, L. Jin, N. Zhou, An update of novel screening methods for GPCR in drug discovery expert opin, Drug Discov. 7 (2012) 791–806.
[5] S. Brogi, A. Tafi, L. Desaubry, C.G. Nebigil, Discovery of GPCR ligands for probing signal transduction pathways, Front. Pharmacol. 5 (2014), http://dx.doi.org/10.3389/fphar.2014.00255.
[6] M. Jo, S.T. Jung, Engineering therapeutic antibodies targeting G-protein-coupled receptors, Exp. Mol. Med. 48 (2016) e207.
[7] K. Miyano, Y. Sudo, A. Yokoyama, K. Hisaoka-Nakashima, N. Morioka, M. Takebayashi, Y. Nakata, Y. Higami, Y. Uezono, History of the G protein-coupled receptor (GPCR) assays from traditional to a state-of-the-art biosensor assay, J. Pharmacol. Sci. 126 (2014) 302–309.
[8] R. Lappano, M. Maggiolini, G protein-coupled receptors: novel targets for drug discovery in cancer, Nat. Rev. Drug Discov. 10 (2011) 47–60.
[9] R.M. Cooke, A.J. Brown, F.H. Marshall, J.S. Mason, Structures of G protein-coupled receptors reveal new opportunities for drug discovery, Drug Discov. Today 20 (2015) 1355–1364.
[10] R.J. Lefkowitz, J. Roth, I. Pastan, Radioreceptor assay of adrenocorticotropic hormone: new approach to assay of polypeptide hormones in plasma, Science 170 (1970) 633–635.
[11] F. Ciruela, K.A. Jacobson, V. Fernandez-Duenas, Portraying G protein-coupled receptors with fluorescent ligands, ACS Chem. Biol. 9 (2014) 1918–1928.
[12] L.A. Stoddart, L.E. Kilpatrick, S.J. Briddon, S.J. Hill, Probing the pharmacology of G protein-coupled receptors with fluorescent ligands, Neuropharmacology 98 (2015) 48–57.
[13] I. Nederpelt, V. Georgi, F. Schiele, K. Nowak-Reppel, A.E. Fernandez-Montalvan, A.P. IJzerman, L.H. Heitman, Characterization of 12 GnRH peptide agonists—a kinetic perspective, Br. J. Pharmacol. 173 (2016) 128–141.
[14] K. Leach, P.M. Sexton, A. Christopoulos, Quantification of allosteric interactions at G protein-coupled receptors using radioligand binding assays, Curr. Protoc. Pharmacol. Chapter 1 (2011). Unit 1 22.
[15] B. Posner, Y. Hong, E. Benvenuti, M. Potchoiba, D. Nettleton, L. Lui, A. Ferrie, F. Lai, Y. Fang, J. Miret, C. Wielis, B. Webb, Multiplexing G protein-coupled receptors in microarrays: a radioligand-binding assay, Anal. Biochem. 365 (2007) 266–273.
[16] J.A. Maynard, N.C. Lindquist, J.N. Sutherland, A. Lesuffleur, A.E. Warrington, M. Rodriguez, S.H. Oh, Surface plasmon resonance for high-throughput ligand screening of membrane-bound proteins, Biotechnol. J. 4 (2009) 1542–1558.
[17] M.J. Lohse, S. Nuber, C. Hoffmann, Fluorescence/bioluminescence resonance energy transfer techniques to study G-protein-coupled receptor activation and signaling, Pharmacol. Rev. 64 (2012) 299–336.
[18] P. Schwille, F.J. Meyer-Almes, R. Rigler, Dual-color fluorescence cross-correlation spectroscopy for multicomponent diffusional analysis in solution, Biophys. J. 72 (1997) 1878–1886.
[19] H. Glauner, I.R. Ruttekolk, K. Hansen, B. Steemers, Y.D. Chung, F. Becker, S. Hannus, R. Brock, Simultaneous detection of intracellular target and off-target binding of small molecule cancer drugs at nanomolar concentrations, Br. J. Pharmacol. 160 (2010) 958–970.
[20] R.A. Cinelli, A. Ferrari, V. Pellegrini, M. Tyagi, M. Giacca, F. Beltram, The enhanced green fluorescent protein as a tool for the analysis of protein dynamics and localization: local fluorescence study at the single-molecule level, Photochem. Photobiol. 71 (2000) 771–776.
[21] Y. Shibata, J.F. White, M.J. Serrano-Vega, F. Magnani, A.L. Aloia, R. Grisshammer, C.G. Tate, Thermostabilization of the neurotensin receptor NTS1, J. Mol. Biol. 390 (2009) 262–277.
[22] K.M. Schlinkmann, A. Honegger, E. Tureci, K.E. Robison, D. Lipovsek, A. Pluckthun, Critical features for biosynthesis, stability, and functionality of a G protein-coupled receptor uncovered by all-versus-all mutations, Proc. Natl. Acad. Sci. USA 109 (2012) 9810–9815.
[23] K.S. Orwig, M.R. Lassetter, M.K. Hadden, T.A. Dix, Comparison of N-terminal modifications on neurotensin (8–13) analogues correlates peptide stability but not binding affinity with in vivo efficacy, J. Med. Chem. 52 (2009) 1803–1813.
[24] K.F. Karpinski, Optimality assessment in the enzyme-linked immunosorbent assay (ELISA), Biometrics 46 (1990) 381–390.
[25] Y. Cheng, W.H. Prusoff, Relationship between the inhibition constant (K_1) and the concentration of inhibitor which causes 50 per cent inhibition (I_{50}) of an enzymatic reaction, Biochem. Pharmacol. 22 (1973) 3099–3108.
[26] E.C. Hulme, M.A. Trevethick, Ligand binding assays at equilibrium: validation and interpretation, Br. J. Pharmacol. 161 (2010) 1219–1237.
[27] H.J. Motulsky, L.C. Mahan, The kinetics of competitive radioligand binding predicted by the law of mass action, Mol. Pharmacol. 25 (1984) 1–9.
[28] C. Dong, C.M. Filipeanu, M.T. Duvernay, G. Wu, Regulation of G protein-coupled receptor export trafficking, Biochim. Biophys. Acta 1768 (2007) 853–870.
[29] D. Ott, R. Frischknecht, A. Pluckthun, Construction and characterization of a kappa opioid receptor devoid of all free cysteines, Protein Eng. Des. Sel. 17 (2004) 37–48.
[30] O. Hegener, L. Prenner, F. Runkel, S.L. Baader, J. Kappler, H. Haberlein, Dynamics of β2-adrenergic receptor–ligand complexes on living cells, Biochemistry 43 (2004) 6190–6199.
[31] S.J. Briddon, B. Kellam, S.J. Hill, Design and use of fluorescent ligands to study ligand–receptor interactions in single living cells, Methods Mol. Biol. 746 (2011) 211–236.
[32] S.J. Briddon, S.J. Hill, Pharmacology under the microscope: The use of fluorescence correlation spectroscopy to determine the properties of ligand–receptor complexes, Trends Pharmacol. Sci. 28 (2007) 637–645.
[33] A. Teichmann, C. Rutz, A. Kreuchwig, G. Krause, B. Wiesner, R. Schulein, The pseudo signal peptide of the corticotropin-releasing factor receptor type 2A prevents receptor oligomerization, J. Biol. Chem. 287 (2012) 27265–27274.
[34] V. Vukojevic, Y. Ming, C. D'Addario, M. Hansen, U. Langel, R. Schulz, B. Johansson, R. Rigler, L. Terenius, μ-Opioid receptor activation in live cells, FASEB J. 22 (2008) 3537–3548.
[35] C. Caballero-George, T. Sorkalla, D. Jakobs, J. Bolanos, H. Raja, C. Shearer, E. Bermingham, H. Haberlein, Fluorescence correlation spectroscopy in drug discovery: study of Alexa532–endothelin 1 binding to the endothelin ETA receptor to describe the pharmacological profile of natural products, Sci. World J. 2012 (2012), http://dx.doi.org/10.1100/2012/524169.
[36] R.H. Rose, S.J. Briddon, S.J. Hill, A novel fluorescent histamine H_1 receptor antagonist demonstrates the advantage of using fluorescence correlation spectroscopy to study the binding of lipophilic ligands, Br. J. Pharmacol. 165 (2012) 1789–1800.
[37] D. Jakobs, T. Sorkalla, H. Haberlein, Ligands for fluorescence correlation spectroscopy on G protein-coupled receptors, Curr. Med. Chem. 19 (2012) 4722–4730.
[38] K. Herrick-Davis, E. Grinde, A. Cowan, J.E. Mazurkiewicz, Fluorescence correlation spectroscopy analysis of serotonin, adrenergic, muscarinic, and dopamine receptor dimerization: The oligomer number puzzle, Mol. Pharmacol. 84 (2013) 630–642.
[39] R. Grisshammer, Purification of recombinant G-protein-coupled receptors, Methods Enzymol. 463 (2009) 631–645.
[40] J. Tucker, R. Grisshammer, Purification of a rat neurotensin receptor expressed in *Escherichia coli*, Biochem. J. 317 (1996) 891–899.
[41] C.A. Sarkar, I. Dodevski, M. Kenig, S. Dudli, A. Mohr, E. Hermans, A. Pluckthun, Directed evolution of a G protein-coupled receptor for expression, stability, and binding selectivity, Proc. Natl. Acad. Sci. USA 105 (2008) 14808–14813.

[42] P. Milovnik, D. Ferrari, C.A. Sarkar, A. Pluckthun, Selection and characterization of DARPins specific for the neurotensin receptor 1, Protein Eng. Des. Sel. 22 (2009) 357–366.
[43] K.M. Schlinkmann, M. Hillenbrand, A. Rittner, M. Kunz, R. Strohner, A. Pluckthun, Maximizing detergent stability and functional expression of a GPCR by exhaustive recombination and evolution, J. Mol. Biol. 422 (2012) 414–428.
[44] B.K. Kobilka, Amino and carboxyl terminal modifications to facilitate the production and purification of a G protein-coupled receptor, Anal. Biochem. 231 (1995) 269–271.
[45] D.M. Rosenbaum, V. Cherezov, M.A. Hanson, S.G. Rasmussen, F.S. Thian, T.S. Kobilka, H.J. Choi, X.J. Yao, W.I. Weis, R.C. Stevens, B.K. Kobilka, GPCR engineering yields high-resolution structural insights into β2-adrenergic receptor function, Science 318 (2007) 1266–1273.
[46] T. Weidemann, P. Schwille, Fluorescence correlation spectroscopy in living cells, in: P. Hinterdorfer, A. van Oijen (Eds.), Handbook of Single-molecule Biophysics, Springer Science+Business Media, New York, 2009, pp. 217–241.
[47] T. Wohland, K. Friedrich, R. Hovius, H. Vogel, Study of ligand–receptor interactions by fluorescence correlation spectroscopy with different fluorophores: evidence that the homopentameric 5-hydroxytryptamine type 3As receptor binds only one ligand, Biochemistry 38 (1999) 8671–8681.
[48] C. Labbe-Jullie, S. Barroso, D. Nicolas-Eteve, J.L. Reversat, J.M. Botto, J. Mazella, J.M. Bernassau, P. Kitabgi, Mutagenesis and modeling of the neurotensin receptor NTR1: Identification of residues that are critical for binding SR 48692, a nonpeptide neurotensin antagonist, J. Biol. Chem. 273 (1998) 16351–16357.
[49] H. Lu, P.J. Tonge, Drug-target residence time: critical information for lead optimization, Curr. Opin. Chem. Biol. 14 (2010) 467–474.
[50] R.A. Copeland, D.L. Pompliano, T.D. Meek, Drug-target residence time and its implications for lead optimization, Nat. Rev. Drug Discov. 5 (2006) 730–739.
[51] S. Nunez, J. Venhorst, C.G. Kruse, Target–drug interactions: first principles and their application to drug discovery, Drug Discov. Today 17 (2012) 10–22.
[52] D. Guo, J.M. Hillger, A.P. IJzerman, L.H. Heitman, Drug-target residence time—a case for G protein-coupled receptors, Med. Res. Rev. 34 (2014) 856–892.
[53] P.J. Harding, H. Attrill, S. Ross, J.R. Koeppe, A.N. Kapanidis, A. Watts, Neurotensin receptor type 1: *Escherichia coli* expression, purification, characterization, and biophysical study, Biochem. Soc. Trans. 35 (2007) 760–763.
[54] I. Navratilova, M. Dioszegi, D.G. Myszka, Analyzing ligand and small molecule binding activity of solubilized GPCRs using biosensor technology, Anal. Biochem. 355 (2006) 132–139.
[55] S.G. Patching, Surface plasmon resonance spectroscopy for characterisation of membrane protein–ligand interactions and its potential for drug discovery, Biochim. Biophys. Acta 1838 (2014) 43–55.
[56] J.L. Swift, M.C. Burger, D.T. Cramb, A quantum dot-labeled ligand–receptor binding assay for G protein-coupled receptors contained in minimally purified membrane nanopatches, Methods Mol. Biol. 552 (2009) 329–341.
[57] J.L. Swift, M.C. Burger, D. Massotte, T.E. Dahms, D.T. Cramb, Two-photon excitation fluorescence cross-correlation assay for ligand–receptor binding: cell membrane nanopatches containing the human μ-opioid receptor, Anal. Chem. 79 (2007) 6783–6791.
[58] D.S. Auld, M.W. Farmen, S.D. Kahl, A. Kriauciunas, K.L. McKnight, C. Montrose, J.R. Weidner, Receptor binding assays for HTS and drug discovery, in: G.S. Sittampalam, N.P. Coussens, H. Nelson, M. Arkin, D. Auld, C. Austin, B. Bejcek, M. Glicksman, J. Inglese, P.W. Iversen, Z. Li, J. McGee, O. McManus, L. Minor, A. Napper, J.M. Peltier, T. Riss, O.J.J. Trask, J. Weidner (Eds.), Assay Guidance Manual, Eli Lilly and National Center for Advancing Translational Sciences, Indianapolis, IN, 2012 [online].
[59] F.M. Heydenreich, Z. Vuckovic, M. Matkovic, D.B. Veprintsev, Stabilization of G protein-coupled receptors by point mutations, Front. Pharmacol. 6 (2015), http://dx.doi.org/10.3389/fphar.2015.00082.
[60] C.L. Piscitelli, J. Kean, C. de Graaf, X. Deupi, A molecular pharmacologist's guide to G protein-coupled receptor crystallography, Mol. Pharmacol. 88 (2015) 536–551.
[61] C.B. Roth, M.A. Hanson, R.C. Stevens, Stabilization of the human β2-adrenergic receptor TM4–TM3–TM5 helix interface by mutagenesis of Glu122(3.41), a critical residue in GPCR structure, J. Mol. Biol. 376 (2008) 1305–1319.
[62] L.T. May, K. Leach, P.M. Sexton, A. Christopoulos, Allosteric modulation of G protein-coupled receptors, Annu. Rev. Pharmacol. Toxicol. 47 (2007) 1–51.
[63] S. Kubetzko, E. Balic, R. Waibel, U. Zangemeister-Wittke, A. Pluckthun, PEGylation and multimerization of the anti-p185HER-2 single chain Fv fragment 4D5: Effects on tumor targeting, J. Biol. Chem. 281 (2006) 35186–35201.
[64] A.J. Leitz, T.H. Bayburt, A.N. Barnakov, B.A. Springer, S.G. Sligar, Functional reconstitution of β2-adrenergic receptors utilizing self-assembling nanodisc technology, BioTechniques 40 (2006) 601–602, 604, 606, passim.
[65] U. Gether, S. Lin, B.K. Kobilka, Fluorescent labeling of purified β2-adrenergic receptor: Evidence for ligand-specific conformational changes, J. Biol. Chem. 270 (1995) 28268–28275.
[66] J.G. Baker, The selectivity of β-adrenoceptor antagonists at the human β1, β2, and β3 adrenoceptors, Br. J. Pharmacol. 144 (2005) 317–322.
[67] M. Isogaya, Y. Sugimoto, R. Tanimura, R. Tanaka, H. Kikkawa, T. Nagao, H. Kurose, Binding pockets of the β_1- and β_2-adrenergic receptors for subtype-selective agonists, Mol. Pharmacol. 56 (1999) 875–885.
[68] S.N. Louis, T.L. Nero, D. Iakovidis, G.P. Jackman, W.J. Louis, LK 204-545, a highly selective β1-adrenoceptor antagonist at human β-adrenoceptors, Eur. J. Pharmacol. 367 (1999) 431–435.
[69] G. Liapakis, W.C. Chan, M. Papadokostaki, J.A. Javitch, Synergistic contributions of the functional groups of epinephrine to its affinity and efficacy at the β2 adrenergic receptor, Mol. Pharmacol. 65 (2004) 1181–1190.
[70] C. Pooput, E. Rosemond, J. Karpiak, F. Deflorian, S. Vilar, S. Costanzi, J. Wess, K.L. Kirk, Structural basis of the selectivity of the β_2-adrenergic receptor for fluorinated catecholamines, Bioorg. Med. Chem. 17 (2009) 7987–7992.
[71] J.L. Benovic, R.G. Shorr, M.G. Caron, R.J. Lefkowitz, The mammalian β2-adrenergic receptor: purification and characterization, Biochemistry 23 (1984) 4510–4518.
[72] F. Richard, S. Barroso, J. Martinez, C. Labbe-Jullie, P. Kitabgi, Agonism, inverse agonism, and neutral antagonism at the constitutively active human neurotensin receptor 2, Mol. Pharmacol. 60 (2001) 1392–1398.
[73] B. Cusack, K. Jansen, D.J. McCormick, T. Chou, Y. Pang, E. Richelson, A single amino acid of the human and rat neurotensin receptors (subtype 1) determining the pharmacological profile of a species-selective neurotensin agonist, Biochem. Pharmacol. 60 (2000) 793–801.
[74] D. Gully, B. Labeeuw, R. Boigegrain, F. Oury-Donat, A. Bachy, M. Poncelet, R. Steinberg, M.F. Suaud-Chagny, V. Santucci, N. Vita, F. Pecceu, C. Labbe-Jullie, P. Kitabgi, P. Soubrie, G. Le Fur, J.P. Maffrand, Biochemical and pharmacological activities of SR 142948A, a new potent neurotensin receptor antagonist, J. Pharmacol. Exp. Ther. 280 (1997) 802–812.
[75] J. Hesselgesser, M. Liang, J. Hoxie, M. Greenberg, L.F. Brass, M.J. Orsini, D. Taub, R. Horuk, Identification and characterization of the CXCR4 chemokine receptor in human T cell lines: ligand binding, biological activity, and HIV-1 infectivity, J. Immunol. 160 (1998) 877–883.
[76] P. Loetscher, J.H. Gong, B. Dewald, M. Baggiolini, I. Clark-Lewis, N-terminal peptides of stromal cell-derived factor-1 with CXC chemokine receptor 4 agonist and antagonist activities, J. Biol. Chem. 273 (1998) 22279–22283.
[77] M.P. Crump, J.H. Gong, P. Loetscher, K. Rajarathnam, A. Amara, F. Arenzana-Seisdedos, J.L. Virelizier, M. Baggiolini, B.D. Sykes, I. Clark-Lewis, Solution structure and basis for functional activity of stromal cell-derived factor-1: dissociation of CXCR4 activation from binding and inhibition of HIV-1, EMBO J. 16 (1997) 6996–7007.
[78] B.J. Doranz, M.J. Orsini, J.D. Turner, T.L. Hoffman, J.F. Berson, J.A. Hoxie, S.C. Peiper, L.F. Brass, R.W. Doms, Identification of CXCR4 domains that support coreceptor and chemokine receptor functions, J. Virol. 73 (1999) 2752–2761.
[79] R. Staudinger, J.C. Bandres, Solubilization of the chemokine receptor CXCR4, Biochem. Biophys. Res. Commun. 274 (2000) 153–156.
[80] B. Wu, E.Y. Chien, C.D. Mol, G. Fenalti, W. Liu, V. Katritch, R. Abagyan, A. Brooun, P. Wells, F.C. Bi, D.J. Hamel, P. Kuhn, T.M. Handel, V. Cherezov, R.C. Stevens, Structures of the CXCR4 chemokine GPCR with small-molecule and cyclic peptide antagonists, Science 330 (2010) 1066–1071.
[81] G. Thoma, M.B. Streiff, J. Kovarik, F. Glickman, T. Wagner, C. Beerli, H.G. Zerwes, Orally bioavailable isothioureas block function of the chemokine receptor CXCR4 in vitro and in vivo, J. Med. Chem. 51 (2008) 7915–7920.
[82] H. Tamamura, A. Hori, N. Kanzaki, K. Hiramatsu, M. Mizumoto, H. Nakashima, N. Yamamoto, A. Otaka, N. Fujii, T140 analogs as CXCR4 antagonists identified as anti-metastatic agents in the treatment of breast cancer, FEBS Lett. 550 (2003) 79–83.